Green Chemistry

Accepted Manuscript

ROYAL SOCIETY OF CHEMISTRY

www.rsc.org/greenchem

Journal Name

ARTICLE

Bifunctional hydrophobic ionic liquids: Facile synthesis by thiol-ene "click" chemistry

Received 00th January 20xx,
Accepted 00th January 20xx

DOI: 10.1039/x0xx00000x

www.rsc.org/

Manuel Sanchez Zayas, Jamie C. Gaitor, Stephen T. Nestor, Samuel Minkowicz, Yinghong Sheng and Arsalan Mirjafari*

We describe the facile, robust and orthogonal fabrication of a structurally comprehensive library of hydrophobic trimethoxysilyl-functionalized ionic liquids with C_7–C_{15} thioether spacer, using thiol-ene "click" chemistry. The synthesized ionic liquids displayed very low glass transition temperatures, high thermal stability and were hydrophobic in character. And the ability to serve as surface coating agents was tested by immobilizing them on the surface of iron oxide supermagnetic nanoparticles and the organic loadings were quantified.

Introduction

Demands for the construction of advanced functional materials with accurately engineered structures and properties have increased significantly with the growing needs to address resource, health, and energy challenges. In addition to the structural requirements for the preparation of the novel materials, scientists have also sought to synthesize them *via* high-yielding, simple to perform, covalent and preferably sustainable chemistry. These motivations in tandem with the recent advances in "click" chemistry have created a growing research area with concentration on robust, efficient, and orthogonal methods for the preparation of new materials in both fundamental and applied fields.[1]

Recently, ionic liquids (ILs) have received a considerable upsurge of interest as green solvents for organic synthesis and separation technologies due to their superior physicochemical properties (*e.g.* effectively non-existing vapor pressure, wide liquid range, low flammability, high ionic and thermal conductivity, wide electrochemical potential window, excellent thermal, chemical and radiochemical stability and exceptional solubility toward many substances, ranging from asphalt to cellulose) over the conventional volatile organic solvents.[2] By incorporating ion-tethered functional groups into the IL structures, an interesting subclass of ILs called task-specific ionic liquids (TSILs),[3] or simply functionalized ILs, has been generated as a new class of materials with unique physicochemical properties. These properties can be customized by selecting the cations and/or anions for specific tasks, ranging from organic synthesis and catalysis to energy, materials and medicine.[4] Particularly, trialkoxysilyl-functionalized ILs have been used for the fabrication of many important materials and devices, including catalyst coated magnetic and mesoporous metal oxides,[5] metal-NHC supported catalysts,[6] organic-inorganic hybrid electrolytes for lithium ion battery,[7] dye-sensitized solar cells,[8] CO_2 capture,[9] nanosilica-based ionogels and nanocamposites,[10] thermally-stable stationary phase for HPLC,[11] electrochromic devices,[12] and transducers.[13]

Due to the nonvolatile nature of ILs, the challenges traditionally associated with their functionalization — quantitative conversion, purification limitations (*e.g.* ineffectiveness of distillation and crystallization methods due to the lack of vapor pressure and their non-crystalline structures) and controlling multiple reaction sites — represent an important opportunity for efficient and functional group tolerant strategies, such as "click" chemistry, to develop concise methodologies for their synthesis. The chemo- and regio-specificity, quantitative yields and orthogonality, that are the hallmarks of click reactions, greatly enable the efficient fabrication of functional ILs *via* the formation of new carbon-heteroatom bonds, which fall within the realm of philosophy of green chemistry.[14]

In this study, we report an efficient and robust photo-initiated thiol-ene chemistry to synthesize a series of tailored, hydrophobic mercaptopropyltrimethoxysilane ILs containing long alkyl spacers (C_7–C_{15}) with low melting points and high thermal stability (Scheme 1). These ILs contain trimethoxysilane moiety as an anchoring group to hydroxylated surfaces such as inorganic oxides, which forms strong covalent siloxane bonds to such surfaces, making them particularly useful for bridging organic and inorganic components. The thiol group, separated by an alkyl spacer (C_3–C_{11}) from the cation, acts as a *"symmetry-breaking"* moiety and imposes a significant depressive effect on the T_m values without sacrificing hydrophobicity, according to our previous report.[15]

[a] *Department of Chemistry and Physics, Florida Gulf Coast University, Fort Myers, Florida 33965, United States. Email: amirjafari@fgcu.edu*

Electronic Supplementary Information (ESI) available: [details of any supplementary information available should be included here]. See DOI: 10.1039/x0xx00000x

Generally, modulation of functionality's reactivity can be expected as a function of the length and structure of the spacers. However, their melting points begin to increase significantly once an *N*-substituted tail exceeds seven carbon atoms for several homologous series of 1-alkyl-3-methylimidazolium ILs.[16] However, we recently reported that it is possible to design 1-methyl-3-thiaalkylimidazolium bistriflimide ILs with alkyl chains as long as 20 carbons while keeping their melting points below room temperature. This was simply achieved by strategically incorporating sulfur atom into the different positions of alkyl side chains *via* thiol-ene reaction in order to incorporate a "kink" into the chains and disrupt packing, similar to natural fatty acids.[15] The trialkoxysilane-functionalized ILs are uniquely amendable to unsymmetrical archetypes by introduction of sulfur atom, which has profound implications on the physicochemical properties of ILs. Furthermore, sulfur functionality enables the formation of an additional coordinative bond with metals that do not readily hydroxylate (*e.g.* Au, Ag and Pt), which have difficulties with coating formation and/or adherence and significantly improves the effectiveness of organosilanes coupling with these less reactive metal substrates.[17]

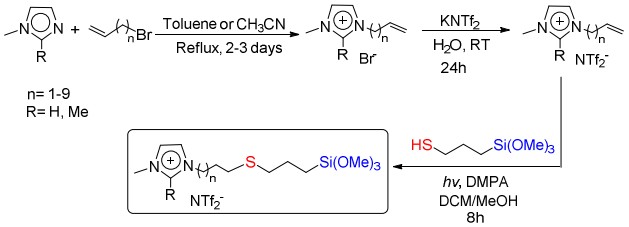

Scheme 1. Two-step preparation of *ene*-bearing ILs as starting materials for the synthesis of imidazolium-type trimethoxysilyl-functionalized ILs with long thioether spacers *via* photo-initiated thiol-ene "click" reaction.

This is the first time that an efficient, robust and orthogonal synthesis of a library of trimethoxysilyl-functionalized ILs (18 examples) with long thioether spacers ($\geq C_7$), while maintaining the liquid state at ambient temperature, is reported. The effects of structural variations on their physicochemical and solvation properties are examined. In addition to their unique physicochemical properties, it was found that the synthesized marcaptosilane ILs can serve as active surface coasting agents. In order to demonstrate that they can be employed as surface-active materials, ILs with different spacer lengths (C_7, C_{11} and C_{15}) were covalently bounded to iron oxide supermagnetic nanoparticles (SPNs) and the IL loadings were quantified by TGA. Also, the role of spacer lengths on the size of SPNs was studied by transmission electron microscopy (TEM).

Experimental Section

Materials and Measurement

For the present study, all of the thiols employed were commercially available in high purity and used without further purification. The photoinitiator (2,2-dimethoxy-2-phenylacetophenone, 99% purity), 1-methylimidazole (98% purity), 1,2-dimethylimidazole (98% purity), triethylamine (99.7%), triphenylphosphine (99%) were purchased from Acros Organics and used without further purification. High purity solvents, such as methylene chloride, methanol and hexanes were purchased from Acros Organics and used without further purification. Potassium bistriflimide, employed for metathesis reactions, was prepared *via* neutralization (pH = 7.0) of $HNTf_2$ (Iolitec GmbH, 80%) with KOH followed by the removal of water.

Characterization of the products using ^1H and ^{13}C was performed on a Bruker 500 MHz NMR with multi-nuclear capabilities using DMSO-d_6. Chemical shifts are reported relative to TMS as the internal reference at 0.00 ppm for both the ^1H and ^{13}C NMR data. ESI-MS analyses were performed by flow-injection on a Thermo Scientific ion trap mass spectrometer using HPLC grade acetonitrile. As our interest was in the cations of these salts, data was collected in positive ion mode. Glass transition temperatures were determined by using a TA Q20 differential scanning calorimeter, with a heating rate of 5 $^oCmin^{-1}$. Thermogravimetric analyses were performed using a TA instrument TGA Q50 under nitrogen flow. Water content of samples was measured by coulometric Karl-Fischer titration C20X from Mettler-Toledo. FT-IR spectra were obtained by using JASCO FT-IR 4600. UV-Visible absorption spectrum was obtained with Shimadzu UV 2450 spectrophotometer, using methylene chloride as solvent. FEI Morgagni 268D TEM used as transmission electron microscopy. Images were captured using an Olympus MegaView III sidemount camera and measured with analySIS® software from ResAlta Research Technologies. Dynamic viscosity and density were measured by Stabinger Viscometer SVM 3000 from Anton-Paar.

General Procedure for the synthesis of *ene*-bearing ILs

As shown in in Scheme 1, *ene*-bearing ILs was synthesized using previously reported procedure from the literature with some slight modification.[15] Briefly, 1 equiv. of 1-methylimidazole/1,2-dimethylimidazole (or triethylamine and triphenylphosphine) was added slowly to 1.1 equiv. of corresponding alkenyl bromide in toluene (Scheme 1, n = 1-3) or acetonitrile (Scheme 1, n = 4-9). The reaction mixture was allowed to stir for 2-3 days under reflux at 110 ^oC and 82 ^oC for toluene and CH_3CN, respectively. The crude product was obtained by evaporating the solvent under reduced pressure, washed it with excess of toluene to remove unreacted starting materials and dried under vacuum to evaporate residual solvents. It was dissolved in H_2O and then added to a solution of 1.1 equiv. of $KNTf_2$ in H_2O and stirred at room temperature for 24 h. After drying, the residue was washed with H_2O three times and dried in vacuum in 70 ^oC for 12 h.

The *ene*-bearing ILs were subjected to standard silver-ion tests to ensure the completeness of the exchange of halide for the NTf_2^- anion. All gave negative results, indicating that residual halide anion content in the salts was below accepted threshold levels.

General Procedure for the synthesis of mercaptopropylsilyl-functionalized ILs

The synthesis of mercaptopropylsilyl-functionalized ILs is shown in Scheme 1. In a dry 150 mL photochemical tube, 1 equiv. of *ene*-bearing ILs was added along with 0.5 equiv. of the photoinitiator 2,2-dimethoxy-2-phenylacetophenone. Minimal amount (<1 mL) of solvent, 1:1 ratio of DCM and MeOH, was added and vigorously stirred until a homogenous solution was obtained. The photochemical tube was capped with a septum, purged with nitrogen, and then sealed with Parafilm. The 3-mercaptopropyltrimethoxysilane (MPTMS) was weighed into a syringe and added through the septum. The contents were stirred briefly and then irradiated with UV for 8h at room temperature under nitrogen atmosphere. The purification process was completed by washing the mixture with hexanes (6 × 30 mL) and dried under vacuum at 70°C for 12h. The IL products **1–16** were isolated as pale yellow liquids in excellent yields (96–>99%).

General Procedure for the synthesis of functionalized magnetite IL–Fe_3O_4 ionogel.

The IL-Fe_3O_4 ionogels were prepared according to a reported procedure with some modifications.[19] In an oven-dried flask, 1 mL of a 3.0 M $FeCl_2$, 2 M HCl solution was mixed with 4 mL of 1.5 M $FeCl_3$, 2 M HCl solution at room temperature. Then, 50 mL of 1.05 M NH_4OH was added dropwise to the solution over a 30 minute period. The dark black suspended particles were separated from aqueous layer and then washed four times with H_2O and then three times with acetone. The collected particles were then left to dry in an oven for 24 hours. Once dried, the particles were crushed, weighed and placed in a glass vial. An equal weight of oleic acid as added to the vial with 1 mL of ethyl acetate per 0.1 g SPNs. Then, the vial was capped and sonicated for 2h at room temperature. The particles were magnetically separated, washed three times with ample amounts of ethyl acetate, followed by three washes with absolute MeOH, and then dried *in vacuo*. The final oleate-coated SPNs (SPNs-OA) nanoparticles were obtained as a dark brown power.

Oleate-coated SPNs (120 mg) and dioxane (60 mL) were added to an oven-dried 100 mL flask. The flask was immediately capped and purged with nitrogen. It was then sonicated for 30 min at room temperature to redisperse SPNs-OA particles. Equal weights of the corresponding silane-functionalized ILs (**1**, **5** and **12**) were added to the flask, placed in a 75 °C oil bath and heated for 48 h with vigorous stirring. The particles were separated by a hand-held rare-earth magnet, washed it with CH_2Cl_2 and acetone three times and then dried under vacuum at 70 °C for 12h.

Results and discussion

Synthesis: A "click" paradigm

In general, the relative hydrolytic instability of trialkoxysilanes and trimethoxysilanes in particular, has significantly restricted the range of useful methods and experimental conditions for their syntheses. Consequently, access to trialkoxysilanes depends upon the limited numbers of approaches. The *N*-alkylation of the 1-methylimidazole with (3-chloropropyl)trimethoxysilane is the most commonly employed method for the preparation of trialkoxysilyl based ILs because of its good to excellent yields and the readily availability of starting materials.[6-12] However, the major limitation of this method is that only hydrophilic trialkoxysilyl-based ILs with short alkyl spacer (C_3) are synthesizable. Han et al. reported Pd(II) immobilized on mesoporous silica using imidazolium-based ILs as NHC ligands, containing an N1-substituted propyltrimethoxysilane group and an N3-bonded alkyl chain with different lengths for the hydrogenation of alkenes and allyl alcohols. Pd(II)-NHC IL with a C_{10} side chain demonstrates the higher selectivity in the hydrogenation of allyl alcohol in comparison to the ILs with C_1 and C_4 side chains and commercial Pd/C as well.[6b] Likewise, according to Alper's report, the N1-propyltrimethoxysilylated ILs with N3-octyl side chain yields better results for the immobilization of Pt on Fe_3O_4 nanoparticles in terms of size of the nanoparticles, compared to the C_3 and C_4 analogues for the selective hydrogenation of α,β-unsaturated aldehydes.[5a] In a different approach, Kadib et al. reported the hydrosilyation of alkenes using the Karsted's catalyst for the preparation of disilyated guanidine ILs. Although the catalyst loading is quite low, it requires an expensive Rh or Pd metal catalyst.[18] In fact, both methods mentioned above have only moderate functional group tolerance and product regioselectivity and require post-synthetic purification steps to remove excess metal/reactants from moisture sensitive products. Not only does our strategy have the potential to overcome many of these drawbacks, but it also provides a facile and robust method to synthesize a library of trimethoxysilyl-functionalized ILs, containing long linear alkyl spacers (C_7–C_{15}) with the sulfur heteroatom strategically placed from C4 to C12. The key objective of this work is to develop a novel series of functional silane ILs that are highly hydrophobic while being low melting salts. Recently, Takamatsu *et al.* reported using the thiol-ene reaction for the construction of mercaptopropylsilane ILs containing the carboxylate anion, paired with different cations to serve as the ionic component in the dielectric layer of a transducer with improved electrostatic attraction between electrodes. In this patent, neither the physicochemical properties, nor the structure-property relationship of these ILs were discussed.[13]

The thiol-ene "click" chemistry can be used to regiospecifically unite *ene*-bearing ILs with 3-mercaptopropyltrimethoxysilane (MPTMS) to afford only linear mercaptoalkyltrimethoxysilyl-functionalized ILs **1–16** (Figure 1). The process is experimentally simple, wide in scope and it was performed using an approach modeled by Garrell et al.[19] In this method, equimolar amounts of *ene*-bearing ILs and MPTMS and 0.5 mol photoinitiator DMPA (2,2-dimethoxy-2-phenylacetophenone) (see ESI, Figure S1) are mixed in the presence of a minimal amount of solvent (1:1 ratio of MeOH/DCM; 0.5-1 mL) and irradiated at room temperature for 8 h. The resulting IL products were formed in high yields with no chromatographic separation required and were simply purified by washing with

hexanes, which none of the starting and product ILs were soluble, to remove small amounts of unreacted MPTMS, and decomposed photoinitiator. As noted, the reaction is operationally simple, oxygen- and water-tolerant conditions, and generate products in high yields with minimal requirements for product purification process, which does not involve the use of halogenated solvents nor chromatographic separation. All are in accordance with the principles of Green Chemistry.

Mirjafari and O'Brien recently reported that the type of solvent has a profound effect on the outcome of thiol-ene reaction. In the presence of a polar protic solvent like MeOH, the regioselectivity of thiol-ene reaction is reversed to afford Markovnikov-oriented products in excellent yields, which led to the formation of ILs with branched thioether lipidic tails that have different physicochemical properties in comparison to their linear counterparts.[20] In order to avoid formation of branched ILs for the work described within, we used 1:1 CH_2Cl_2/MeOH ratio. On the basis of ^1H and ^{13}C NMR, and MS, no Markovnikov-oriented (branched) products were obtained during the course of this study.

Using small quantities of photoinitiator relative to alkene (mol/mol) in this reactions, did not lead to the satisfactory results under air or nitrogen, prompting us to considerably increase the amount photoinitiator (10 times more than amount reported in Ref. 19). There was no significant difference in outcomes whether the reactions were conducted under nitrogen or air.

The scope of the study was expanded to ILs with imidazolium and ammonium cations bearing multiple *ene* groups. Reacting these ILs with additional amounts of MPTMS under the same reaction conditions led to the quantitative formation of the desired polyadducts (Figure 1, IL **14**) and were isolated in excellent yields. However, the synthesis of IL **14** required a longer irradiation time and additional amounts of photoinitiator to achieve satisfactory product yields.

A series of *ene*-bearing ILs containing C_3–C_{11} side chains including imidazolium, ammonium and phosphonium cations can be quantitatively clicked with MPTMS to form the 17 examples of structurally comprehensive mercaptopropyltrimethoxysilane ILs (Figure 1, **1–16**). The synthesis of imidazolium-based *ene*-bearing ILs from the *N*-alkylation of imidazole with alkenyl bromide, followed by metathesis with $KNTf_2$, is shown in Scheme 1. This process is extensively studied as a standard procedure for the preparation of ILs with a high product yields in each step.[16a] Imidazolium-based ILs are an extensively studied class of materials because of the relatively low reagent costs and ease of functionalization. The C2-position of imidazolium-based ILs has an acidic proton, which favors hydrogen bonding with anions and discourages the formation of higher melting point ILs. Ammonium and phosphonium cations are commonly used in ILs structures because of their ease of customization and control over physicochemical properties;[21] in addition, phosphonium salts show very high thermal stability.[22] Therefore, the strategy employed in this study involved the design of hydrophobic ILs with low melting points, containing a variety of cations and could be readily functionalized and purified. Also, the hydrophobicity of ILs can be controlled by inclusion of additional nonpolar moieties into their structures. Typical non-coordinating, hydrophobic bis(trifluoromethane-sulfonyl)imide [NTf_2^-] anion, which is highly stable from both thermal and hydrolytic standpoints, was used.

Both the ^1H and ^{13}C NMR spectra of each **1–16** clearly illustrate complete hydrothiolation, which was readily ascertained on the basis of ^1H NMR peak integration and the disappearance of the olefinic peaks of the starting cations. This was further confirmed by their ESI-MS spectra. Despite extensive work, an X-ray crystal structure was not obtained for ILs **1** and **15**, paired with [BPh_4^-] anion, most likely because trimethoxysilane group diminishes the crystallinity of ILs.

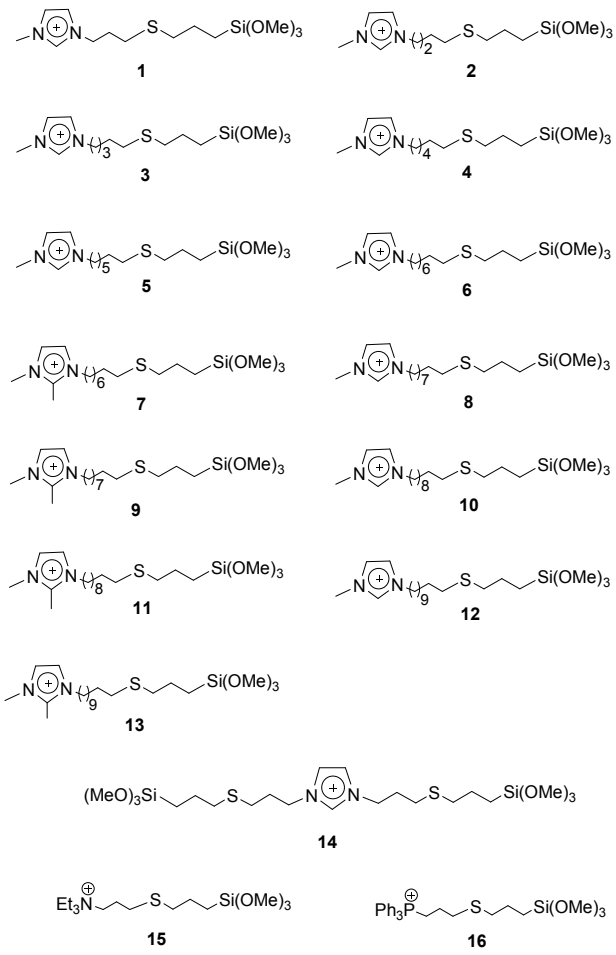

Figure 1. Cation Structures of trimethoxysilane-functionalized ILs (the anion, [NTf_2^-], is not shown), resulting from photoinduced thiol-ene "click" reaction of *ene*-bearing ILs with 3-mercaptopropyltrimethoxysilane.

MPTMS was chosen as a silane precursor for the thiol-ene reaction due to its superior reactivity for surface coating relative to other alkylsilanes, combined with its commercial availability at a low cost. It coupled successfully to *ene*-bearing

ILs with no evidence of hydrolysis of the trimethoxysilane group or cocondensation to form silane dimers. Therefore, we studied the simplicity and feasibility of scaling up the thiol-ene coupling of [allylmim][NTf_2] (Scheme 1, n = 1, R = H) with MPTMS in order to resynthesize IL **1** on a >10 g scale. This reaction was selected because of the relatively low cost of starting materials and similarity of IL **1** to one the few commercially available mercaptosilanes.[23] Following UV irradiation of reactants for 8h, the reaction reached complete conversion (measured by ^{1}H, ^{13}C NMR) and the obtained isolated yield is 91%, which is slightly lower than small scale reaction.

Thermophysical properties and solubility: Structure-property relationships study

The thermophysical properties including phase transition behavior and thermal stability of these 16 new ILs were studied using differential scanning calorimetry (DSC) and thermal gravimetric analysis (TGA), and results compiled to create Table 1. No melting or glass transition temperatures were detected upon heating to 150 °C and cooling to -80 °C, for the synthesized ILs, except IL **15** where their glass transition temperatures (T_g; midpoints of phase transitions) is 23.05 °C.

The phase transition temperature of ILs is controlled by three major factors: intermolecular forces, molecular symmetry and the conformational degrees of the freedom.[24] Our previous report dictates that the total number of carbon atoms and asymmetry of the cations govern the phase transition temperature of ILs.[20] Indeed, the $Si(OMe)_3$ group is the main structural feature of the new ILs that appears to have an substantial influence upon lowering the phase transitions by adding a degree of asymmetry. Another likely explanation for the observed complete disappearance of crystallinity and very low T_g values is that the heightened rotational freedom of the long chains reduces lattice energy of the ILs, leading to the situation in which high chain flexibility predominates over the polarity of trimethoxysilane group. In this context, Jovanovski et al. reported a very low T_g value of -64.4 °C for 1-methyl-3-[3-(trimethoxysilyl)propyl]-imidazolium iodide, which illustrates that the depression in the glass transition point brought about by the inclusion of a $Si(OMe)_3$ moiety is substantial regardless of the nature of the anion.[25] Typically, the rotational disordered state of the bis(trifluoromethanesulfonyl)imide [NTf_2] anion in crystalline salts leads to the considerable T_m/T_g depression, in comparison to halogen anions. Moreover, Rothenberg *et al.* have proposed the former domain constitutes a symmetry-breaking region, the impact of which is eventually outweighed by that of the cumulative inter-chain dispersion forces of progressively longer alkyl groups.[24] Using cues from biology, O'Brien et al. demonstrated that strategic inclusion of a sulfur heteroatom into the symmetry-breaking region of alkyl chains has a profound depressive effects on the T_m/T_g values of amphiphile ILs by imparting a "kink" into the chains and disrupt packing.[15] Overall, the explanation for the lack of packing efficiency of the crystal lattice in the structures of the synthesized ILs and their very low T_g values (less than -80 °C) is a combination of following factors: a) instruction of asymmetry by incorporation of the sulfur and trimethoxysilane groups, b) "kink" effect produced by the sulfur heteroatom, c) charged-diffused, relatively large imidazolium cations and d) effective charge distribution of the NTf_2^- anion.

IL **16**, as a functionalized alkyltriphenylphosphonium salt, showed the highest T_g (23.05 °C) in this series. Inclusion of the sulfur and trimethoxysilane groups into the allytriphenylphosphonium-based IL converts a crystalline solid salt to an amorphous IL, which is liquid at room temperature.

Table 1. Thermophysical properties of ILs synthesized in this study

IL	MW/gmol^{-1}	T_g/°C[a]	$T_{onset5\%}$/°C[b]
1	599.65	<-80	245.81
2	613.68	<-80	263.69
3	627.70	<-80	326.58
4	641.73	<-80	365.38
5	655.76	<-80	342.11
6	669.79	<-80	323.99
7	683.81	<-80	338.01
8	683.81	<-80	342.26
9	697.84	<-80	330.62
10	697.84	<-80	336.97
11	711.87	<-80	321.79
12	711.87	<-80	306.95
13	725.89	<-80	341.61
14	618.74	<-80	330.92
15	711.84	23.05	313.33
16	822.02	<-80	274.90

[a]T_g = glass transition temperature. [b]Temperature at which 5 wt % loss of ILs is observed.

The thermal decomposition temperature ($T_{onset5\%}$) was determined using thermal gravimetric analysis (TGA) and evaluated at 5% mass loss of the samples. $T_{onset5\%}$ values substantially varied between the new ILs, as the exhibited 5% weight loss between 245.81 °C and 365.38 °C, as shown in Table 1. The thermal stability of the mercaptosilane ILs were found to be notably greater than those have been observed for many traditional ILs (1-alkyl-3-methylimidazolium-based ILs typically have thermal stabilities ranging from 145–185 °C[16a]). Among these compounds, IL **4** exhibited the highest thermal stability having $T_{onset5\%}$ of 365.38 °C, which may be one the highest thermal stability for organic compounds. Although a C–S bond is more thermally labile relative to a C–C bond,[26] we observed that the $T_{onset5\%}$ of IL **4** is higher than that of the corresponding all-carbon reference compound, [C_{10}mim][NTf_2],[27] ($\Delta T_{onset5\%}$ of ~65.38 °C) due to excellent thermal stability of trimethoxysilane group.

As shown by Sharma et al., cation-tethered functional groups are able to significantly impact the solvent parameters of ILs (Abraham parameter), which in turn have profound influence on the bulk properties of the materials.[28] To provide further insight into structure-property relationship of the new ILs and their bulk properties, dynamic viscosity (η) and density (ρ) of a representative IL (**1**) were measured as function of

temperature at 1 bar and are shown in Figure 2 graphically and Table S1 (see ESI). The obtained data was compared with the corresponding all-carbon and thioether references with the same number of side-chain backbone atoms (Table 2). As anticipated, the incorporation of sulfur and trimethoxysilane functionalities has great influence on the viscosity of IL **1** in comparison to ILs with alkyl and thioether-containing structural counterparts. For instance, $[C_7C_1im][NTf_2]$, with its saturated all-carbon side chain, has a η value of 77.25 mPa·s at 20 °C[29] but the replacement of its C4 methylene unit with a sulfur atom provides its thioether counterpart with the η value of 149.9 mPa·s at 20 °C.[30] ($\Delta\eta = 72.2$ °C). Likewise, as shown in Table 2, introduction of trimethoxysilane functionality to form IL **1** increased the η value to 201.5 mPa·s at 20 °C, which is greater than the dynamic viscosity of its reference compounds ($\Delta\eta = 124.3$ °C and 51.6 °C for Entries 1 and 2 of Table 1, respectively). Both of these trends are consistent with increased inter-particle interaction brought upon by the grafting of powerfully associating functional groups. For many ILs, viscosity is a strong function of temperature near room temperature, as is the case for the representative IL, with viscosity varying over 7 orders of magnitude in the temperature range studied (Figure 2).

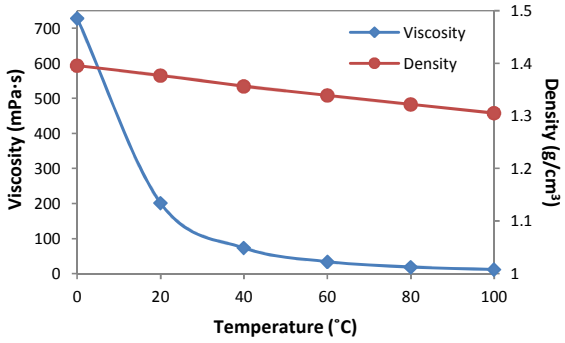

Figure 2. The dynamic viscosity (◆) and density (●) of IL **1** from 0 to 100 °C.

Generally, the ILs' density was found to be dependent to the nature of anion (1-alkyl-3-methylimidazolium ILs with $[NTf_2^-]$ anion has the greater density among other common anions[16a]) and to increase with increasing the length of hydrocarbon chain linkage. However, the density of the IL **1** is slightly lower compared to its thioether analogue (Figure 2 and Tables 2). As is typical, the densities of each compound decreases slightly with temperature, as the compounds are liquids far removed from their critical points.

The miscibility of ILs with both water (polar) and hexanes (nonpolar) solvents was evaluated. The low water solubility observed for the synthesized ILs (less than 0.20% w/v) makes them ideal hydrophobic compounds. Increasing the length of spacers led to the decreasing of their water content. In addition, these ILs are insoluble at 0.1% (w/v) in hexanes. Indeed, the fact that these ILs are immiscible both in water and hexanes can be a further added to their usefulness (see ESI, Figure S2).[31]

Table 2. Comparative dynamic viscosity and density of IL **1** and its alkyl and thioether analogs at 20 °C.

Row	IL	η (mPa·s)[a]	ρ (g/cm^3)[b]	Ref.
1	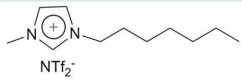	77.2	1.34	29
2	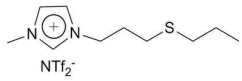	149.9	1.47	30
3	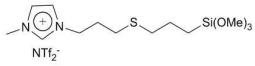	201.5	1.38	—

[a] η = Dynamic viscosity. [b] ρ = Density

Computational modeling and simulation

Molecular modeling can be a useful tool to establish both qualitative and quantitative relations between the properties of ILs and their structures. The molecular modeling was conducted using IL **1** as the model. The structure of **1** was optimized using the B3LYP exchange–correlation functional[32] and the 6-311++G (d,p) basis set as implemented in the Gaussian09 suite of programs.[33] Stable structures were confirmed by computing analytic vibrational frequencies. Figure 3 shows the most stable conformation for IL **1** and its C_7 reference compound with an all-hydrocarbon spacer. Only front-conformations were obtained, while no top conformation was found due to the presence of the flexibility of the bulky NTf_2 anion. The study also indicates a nonbonded interaction (C—H···N hydrogen bond; 1.9795 Å) between the anion and the acidic hydrogen at C2 position of the imidazolium ring. In addition, the electron density isosurface of IL **1** and the all-carbon reference IL are shown in the electrostatic potential energy map in Figure 1. The ESP mapping illustrates the polarization of the cation with the imidazolium ring as the blue region and $Si(OMe)_3$ and S groups as the regions with least positive charge region on the cation (yellow colored) (Figure 3d). Clearly, the negative charge is located on the formal anion (red colored).

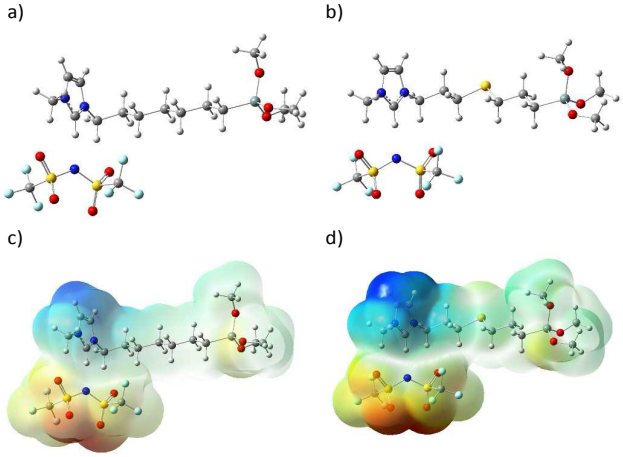

Figure 3. a) The optimized structure of reference IL with an all-carbon spacer at the B3LYP/6-311++G(d,p) level. b) The optimized structure of IL **1** at the B3LYP/6-311++G(d,p) level. c) The electrostatic potential energy map of reference IL with an

all-carbon spacer. d) The electrostatic potential energy map of IL **1**.

All inter-ion interactions were taken into account by explicitly modeling the entire liquid structure using DFT computations of the highest occupied molecular orbital (HOMO) and lowest unoccupied molecular orbital (LUMO) energies. Figure 4 shows the MO patterns of the HOMO and the LUMO of the all-carbon reference IL (a and b) and IL **1** (c and d). The HOMO orbital in the structure of reference IL is more localized on the nitrogen and oxygen atoms of the [NTf_2^-] anion (Figure 4a), while the LUMO orbital is localized on the imidazolium ring (Figure 4b) and the HOMO–LUMO gap is 5.96 eV. In contrast, the HOMO orbital of IL **1** is localized on the sulfur atom (Figure 4c) and the LUMO orbital is on the imidazolium cation similar to the reference IL (Figure 4d). In IL **1**, the HOMO–LUMO gap is reduced to 4.50 eV, likely due to the intramolecular transition in IL **1** versus intermolecular transition in the case of reference IL.

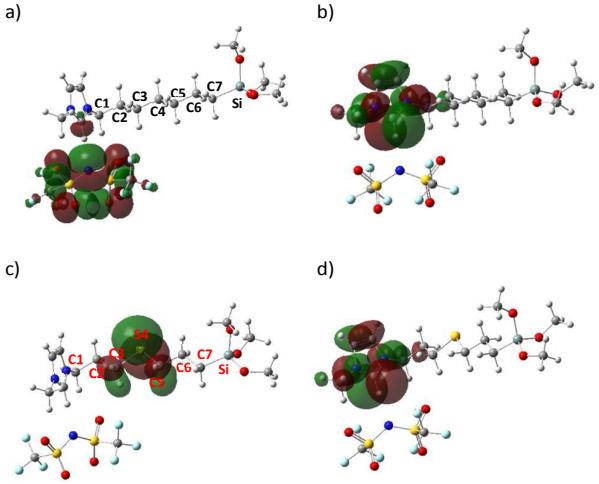

Figure 4. Molecular orbitals of HOMO and LUMO of C_7 reference compound with an all-carbon spacer (a and b, respectively). Molecular orbitals of HOMO (c) and LUMO of IL **1** (d).

In Figure 5, the conformational-energy landscapes of the [C_6mim] cation and its ether and thioether counterparts are depicted as a function of dihedral angle of C2–C3–X4–C5 and C3–X4–C5–C6 (X = C, O or S), relative to the angle at the energy maxima. The results of the calculations are nearly identical to the previously reported calculations for atomic-level structures of *n*-pentane and its heteroatom analogues,[15] demonstrating that the energy barrier between *gauche* and *anti* conformations of the thioether analogue is lower than that of the ether and hydrocarbon counterparts. This energy gap is because of the difference in bonds length of C–S and C–C (184 pm *vs.* 153 pm) and also C–S–C bond angles relative to C–C–C angles (~99° *vs.* ~109°). Considering the rotation of both C–S bonds, the thiaalkyl chain has seven low-energy conformation[15] that imply the "kink" effect into the structures of thioether linkages. Consequently, the high population of kinked chains leads to the substantial melting point depression of the long-chain ILs.

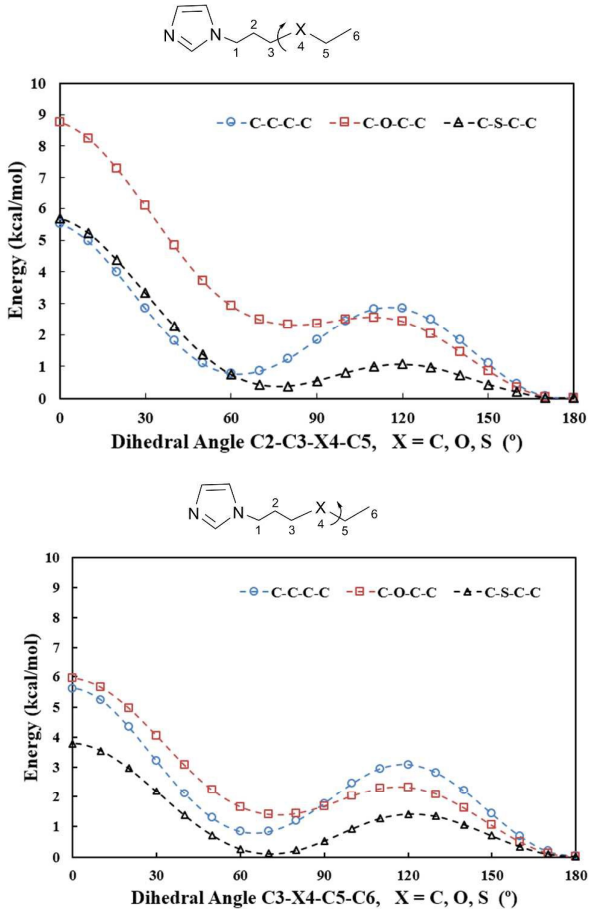

Figure 5. Relative conformational-energy landscape of the imidazolium cation with C_6 side chains for the rotation about the C2–C3–X4–C5 (left) and C3–X4–C5–C6 (right) where the X = C, O and S.

Surface coating applications: Ionogel formation

Recently, preparation, stabilization and functionalization of inorganic nanoparticles with ILs have been considerably studied.[34] A subclass of hybrid materials called ionogels are formed by incorporating ILs on a variety of inorganic supports including silica nanoparticles, metal/metal oxide nanomaterials, polymers, gelators and carbon nanotubes. As a novel class of materials, they are broadly used in the fields of immobilized catalysts, dye-synthesized solar cells, supercapacitors, solid electrolyte-gated organics and drug delivery.[35,36] Ionogels are a class of hybrid materials that combine the properties of ILs with organic/inorganic solid host networks in order to obtain the solid and malleable materials while retaining the unique properties of the IL including large electrochemical window, high specific capacitance, and high ionic conductivity. Importantly, by adjusting the interaction between the ILs guest and their hosts *via* the strategic introduction of different functionalities in ILs,

task-specific ionogels can be formed, which are tailored for specific applications.

The feasible incorporation of functionalized ILs into the structure of inorganic frameworks could induce accurate control over surface properties by modification of the hydrophilic/hydrophobic profile, alteration of the surface activity and adjustment of the bulk properties of these hybrid materials. In this respect, the synthesized silane-functionalized ILs were found to be active surface coating agents and were successfully bounded to the cations on the surface of magnetite supermagnetic Fe_3O_4 nanoparticles (SPNs) to form a novel class of hydrophobic ionogels as shown in Scheme 2. Supermagnetic Fe_3O_4 is one the most widely used nanosupports for anchoring of the silane ligand guests due to its high surface area and the presence of OH groups in the addition of advantageous facile separation. Furthermore, magnetic nanoparticles are distinguished as highly stable and low toxicity materials that have gained increasing attention in many catalytic[34a] and biological[35] fields.

In this study, we first prepared magnetite nanoparticles *via* co-precipitation of Fe (II) and Fe (III) salts in a basic solution, according to Massart's methods.[37] Typically, Fe_3O_4 magnetic nanoparticles prepared *via* this method are characterized with a diameter of 5–15 nm, as confirmed by TEM analysis. These magnetic nanoparticles are slightly soluble in protic solvents and have the tendency to agglomerate to decrease their high surface energy that emerges from the high surface area to volume ratio.

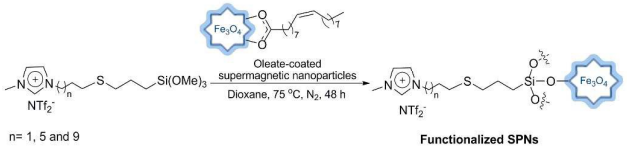

Scheme 2. Preparation of functionalized magnetite SPNs with trimethoxysilyl-based ILs.

To verify that the synthesized ILs could be used as surface coating agents, ILs **1**, **5** and **12** were supported on bare SPNs (IL **1**@SPNs, IL **5**@SPNs and IL **12**@SPNs) and magnetite supermagnetic Fe_3O_4 nanoparticles coated with oleate (IL **1**@SPNs-OA, IL **5**@SPNs-OA and IL **12**@SPNs-OA). Oleate coated SPNs were heated at 75°C in dioxane for 48h. After particle isolation with a hand-held rare earth magnet and rinsing with acetone three times, the resulting constructs were characterized by TGA, TEM and FT-IR spectroscopy (For FT-IR and TEM data, see ESI, Figures S5 and S6). According to the obtained data, the particle size and particle loading are considerably dependent upon the spacer lengths.

TG analysis was conducted to prove the existence of the ILs part in the hybrid nanoparticle structures and the results show that all six compounds had mass loss around 100 °C because of desorbed inner water molecules. Further mass loss at higher temperature was related to the elimination of ILs, immobilized on the surface of Fe_3O_4 nanoparticles. The loading of the ILs **1**, **5** and **12** on bare SPNs were 5.15 wt%, 16.39 wt% and 4.56 wt%, respectively (see ESI, Figure S3). On the other hand, magnetite SPNs coated with oleate demonstrated significantly higher IL loading compared to the bare SPNs (IL **1**@SPNs-OA = 39.81 wt%; IL **5**@SPNs-OA = 31.29 wt%; IL **12**@SPNs-OA = 27.40 wt%) (Figure 6). In this case, the IL **1** with C_7 spacer has profoundly higher IL loading. The plausible reasons for the loading variability is difference in ILs' solubility in dioxan and interaction between ILs and oleate moiety on SPNs.

The size of individual nanoparticles was measured by transmission electron microscopy (TEM), which indicates average sizes of 6.74 ± 0.63, 10.12 ± 0.33 and 9.23 ± 0.41 nm for the IL **1**@SPNs-OA, IL **5**@SPNs-OA and IL **12**@SPNs-OA, respectively (see ESI, Figure S6).

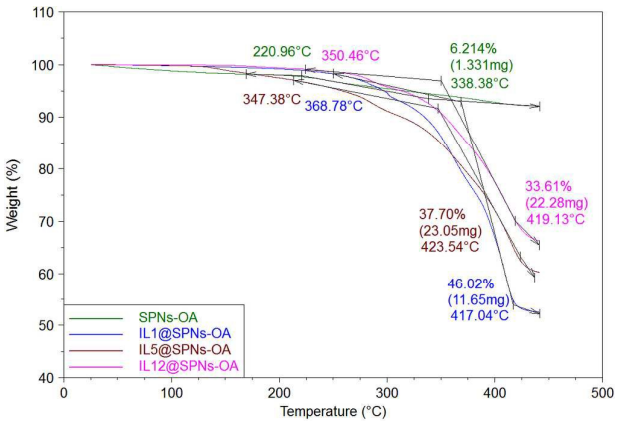

Figure 6. TGA curves of supported ILs on magnetite SPNs coated with oleate (IL **1**@SPNs-OA = 39.81 wt%; IL **5**@SPNs-OA = 31.29 wt%; IL **12**@SPNs-OA = 27.40 wt%)

Conclusions

In summary, the thiol-ene "click" transformation described here is a high-yielding and simplistic fusion process, leading to a series of hydrophobic, multifunctionalized ILs containing long thioether spacers (C_7–C_{15}) with low melting points and high thermal stability. The process exhibits broad scope and provides a series of imidazolium, ammonium and phosphonium-based mercaptosilyl-functionalized ILs (16 examples) in excellent yields and exclusive anti-Markovnikov regioselectivity. In addition, the reaction can be scaled-up simply without sacrificing the product's yield or purity. In order to aid in defining their practical range of use in various applications, the thermophysical properties of the new ILs such as glass transition temperature, decomposition temperature, viscosity and density along with their water contents, were studied. The mercaptosilane class of ILs can have important applications due to their hydrophobicity, moderately low viscosities, high thermal stabilities and wide liquids range. The synthesized ILs were found to be active surface coating agents and were successfully immobilized on magnetite SPNs.

The ability to introduce trimethoxysilane into the structures of ILs would open new horizons for their applications such as surface modification and hybrid materials. The incorporation of a thiol group to the structure of silane-functionalized ILs

could be utilized to construct novel organic-inorganic materials due to strong affinity of thiols to specific metallic surfaces.

Acknowledgements

A.M. and M.S.Z. gratefully acknowledge the generous support from the Alice and Karl Sheffield Scholarship. A.M. also thank Ms. Mobarrez at Arthrex Inc. for experimental assistance and Dr. O'Brien at USA for insightful comments. We acknowledge Department of Chemistry of USF for providing NMR Spectroscopy service. Dr. Kavallieratos and Dr. Govor at FIU are thanked for performing ^{29}Si NMR experiment.

Notes and references

1 R. K. Iha, K. L. Wooley, A. M. Nyström, D. J. Bruke, M. J. Kade and C. J. Hawker, *Chem. Rev.*, 2009, **109**, 5620.
2 (a) T. Welton, *Chem. Rev.*, 1999, **99**, 2071; (b) P. Wasserscheid and T. Welton (Eds), *Ionic Liquids in Synthesis*, Wiley-VCH Verlag, Weinheim, 2008; (*c*) J. P. Hallett and T. Welton, *Chem. Rev.*, 2011, **111**, 3508.
3 J. H. Davis Jr., *Chem. Lett.*, 2004, **33**, 1072.
4 (a) P. S. Kulkarni and C. A. M. Afonso, *Green Chem.,* 2010, **12**, 1139; (b) R. Ferraz, L. C. Branco, C. Prudêncio, J. P. Noronha and Ž. Petrovski, *ChemMedChem*, 2011, **6**, 975; (c) S. Tang, G. A. Baker and H. Zhao, *Chem. Soc. Rev.*, 2012, **41**, 4030; (d) A. Brandt, J. Gräsvik, J. P. Hallett and T. Welton, *Green Chem.*, 2013, **15**, 550; (e) D. R. MacFarlane, N. Tachikawa, M. Forsyth, J. M. Pringle, P. C. Howlett, G. D. Elliott, J. H. Davis, M. Watanabe, P. Simon and C. A. Angell, *Energy Environ. Sci.*, 2014, **7**, 232.
5 (a) R. Abu-Reziq, D, Wang, M. Post and H. Alper, *Adv. Synth. Catal.,* 2007, **349**, 2145; (b) J. Wang, B. Xu, H. Sun and G. Song, *Tetrahedron Lett.,* 2013, **54**, 238.
6 (a) B. Karimi and D. Enders, *Org. Lett.,* 2006, **8**, 1237; (b) G. Liu, M. Hou, T. Wu, T. Jiang, H. Fan, G. Yang and B. Han, *Phys. Chem. Phys. Chem.,* 2011, **13**, 2062.
7 Y. Lu, K. Korf, Y. Kambe, Z. Tu and L. A. Archer, *Angew. Chem. Int. Ed.,* 2014, **53**, 488.
8 E. Stathatos, V. Jovanovski, B. Orel, I. Jerman and P. Lianos, *J. Phys. Chem. C.,* 2007, **111**, 6528.
9 J. M. Zhu, F. Xin, Y. C. Sun and X. C. Dong, *Theor. Found. Chem. Eng.,* 2014, **48**, 787.
10 S. S. Moganty, S. Srivastava, Y. Lu, J. L. Scaefer, S. A. Rizvi and L. A. Archer, *Chem. Mater.* 2012, **24**, 1386.
11 M. Zhang, J. Chen, H. Qiu, A. K. Mallik, M. Tkafuji and H. Ihara, *RSC Adv.,* 2014, **4**, 34654.
12 A. Šurca Vuk, V. Jovanovski, A. Pollet-Villard, I. Jerman and B. Orel, *Sol. Energ. Mater. Sol. Cells*, 2008, **92**, 126.
13 S. Takamatsu, R. Matsuno, S. Kumagai, Y. Kokubo, K. Hashimoto, H. Yoshikawa, A. Takahara and H. Otsuka, US 20140300247, 2014.
14 For general aspects of click chemistry, see: (a) H. C. Kolb, M. G. Finn and K. B. Sharpless, *Angew. Chem. Int. Ed.,* 2001, **40**, 2004 and references therein.
15 R. A. O'Brien, A. Mirjafari, K. M. Mattson, S. M. Murray, N. Mobarrez, E. A. Salter, A. Wierzbicki, J. H. Davis Jr. and K. N. West, *J. Phys. Chem. B*, 2014, **118**, 10232.
16 (a) J. L. Anderson, R. Ding, A. Ellern and D. W. Armstrong, *J. Am. Chem. Soc.,* 2005, **127**, 593; (b) A. Mirjafari, R. A. O'Brien, S. M. Murray, K. M. Mattson, N. Mobarrez, K. N. West and J. H. Davis Jr., *ACS Symp. Ser.*, 2012, **9**, 199.
17 (a) B. S. Lee, Y. S. Chi, J. K. Lee, I. S. Choi, C. E. Song, S. K. Namgoong and S. Lee, *J. Am. Chem. Soc.,* 2004, **126**, 480; (b) X. Ma, J. Li, M. Sheu, A. Righter and A. Gilmore, US 2015/014033 A1, 2015.
18 A. El Kadib, P. Hesemann, K. Molvinger, J. Brandner, C. Biolley, P. Gaveau, J. J. E. Moreau and D. Brunel, *J. Am. Chem. Soc.,* 2009, **131**, 2882.
19 A. K. Tucker-Schwartz, R. A. Farrell and R. L. Garrell, *J. Am. Chem. Soc.,* 2011, **133**, 11026.
20 A. Mirjafari, R. A. O'Brien, K. N. West and J. H. Davis Jr., Chem.– *Eur. J.,* 2014, **20**, 7576.
21 D. M. Eike, J. F. Brenneke and E. J. Maginn, *Green Chem.,* 2003, **5**, 323.
22 C. G. Cassity, A. Mirjafari, N. Mobarrez, K. J. Strickland, R. A. O'Brien and J. H. Davis Jr., *Chem. Commun*., 2013, **49**, 7590.
23 3-(2-pyridylethyl)thiopropyltrimethylsilane (SIP6926.2) sold by Gelest Inc.
24 I. Lopez-Martin, E. Burello, P. N. Davey, K. R. Seddon and G. Rothenberg, *ChemPhysChem,* 2007, **8**, 690.
25 V. Jovanovski, B. Orel, R. Ješe, G. Mali, E. Stathatos and P. Lianos, *Int. J. Photoenergy,* 2006, **2006**, 1.
26 J. A. Kerr, *Chem. Rev.,* 1966, **66**, 465.
27 P. S. Kulkarni, L. C. Branco, J. G. Crespo, M. C. Nunes, A. Raymundo and C. A. M. Afonso, *Chem.–Eur. J.,* 2007, **13**, 8487.
28 N. K. Sharma, M. D. Tickell, J. L. Anderson, J. Kaar, V. Pino, B. F. Wicker, D. W. Armstrong, J. H. Davis Jr. and A. J. Russell, *Chem. Commun.,* 2006, 646.
29 T. Mandai, M. Imanari and K. Nishikawa, *Chem. Phys. Lett.*, 2011, **507**, 100.
30 R. A. O'Brien, A. Mirjafari, V. Jajam, E. N. Capley, A. C. Stenson, K. N. West and J. H. Davis Jr., *Tetrahedron Lett.*, 2011, **52**, 5173.
31 (a) G. -T. Wei, Z. Yang, C. -Y. Lee, H. -Y. Yang, C. R. Wang and *J. Am. Chem. Soc.* 2004, **126**, 5036; (b) H. Itoh, K. Naka and Y. Chujo, *J. Am. Chem. Soc.* 2004, **126**, 3026; (c) P. Cui, H. He, D. Chen, H. Liu, S. Zhang, and J. Yang, *Ind. Eng. Chem. Res.*, 2014, **53**, 15909.
32 (a) A. D. Becke, *J. Chem. Phys.,* 1993, **98**, 5648; (b) W. Yang and R. G. Parr, *Phys. Rev. B: Condens. Matter,* 1988, **37**, 785; (c) P. J. Stephens, F. J. Devlin, C. F. Chabalowski and M. J. Frisch, *J. Phys. Chem.,* 1994, **98**, 11623.
33 Gaussian 09, Revision D.01, M. J. Frisch, G. W. Trucks, H. B. Schlegel, G. E. Scuseria, M. A. Robb, J. R. Cheeseman, G. Scalmani, V. Barone, B. Mennucci, G. A. Petersson, H. Nakatsuji, M. Caricato, X. Li, H. P. Hratchian, A. F. Izmaylov, J. Bloino, G. Zheng, J. L. Sonnenberg, M. Hada, M. Ehara, K. Toyota, R. Fukuda, J. Hasegawa, M. Ishida, T. Nakajima, Y. Honda, O. Kitao, H. Nakai, T. Vreven, J. A. Montgomery, Jr., J. E. Peralta, F. Ogliaro, M. Bearpark, J. J. Heyd, E. Brothers, K. N. Kudin, V. N. Staroverov, R. Kobayashi, J. Normand, K. Raghavachari, A. Rendell, J. C. Burant, S. S. Iyengar, J. Tomasi, M. Cossi, N. Rega, J. M. Millam, M. Klene, J. E. Knox, J. B. Cross, V. Bakken, C. Adamo, J. Jaramillo, R. Gomperts, R. E. Stratmann, O. Yazyev, A. J. Austin, R. Cammi, C. Pomelli, J. W. Ochterski, R. L. Martin, K. Morokuma, V. G. Zakrzewski, G. A. Voth, P. Salvador, J. J. Dannenberg, S. Dapprich, A. D. Daniels, Ö. Farkas, J. B. Foresman, J. V. Ortiz, J. Cioslowski and D. J. Fox, Gaussian, Inc., Wallingford CT, 2009.
34 (a) Y. Jun, J. Choi and J. Cheon, *Chem. Commun*., 2007, 1203; (b) J. Dupont and J. D. Scholten, *Chem. Soc. Rev.,* 2010, **39**, 1780; (c) Z. Ma, J. Yu and S. Dai, *Adv. Mater*., 2010, **22**, 261.
35 M. H. Valkenberg, C. deCastro and W. H. Holderich, *Green Chem.* 2002, **4**, 88.
36 (a) D. L. Graham, H. A. Ferreira and P. P. Freitas, *Trends Biotechnol.,* 2004, **22**, 455; (b) T. Neuberger, B. Schopf, H. Hofmann, M. Hofmann and B. von Rechenberg, *J. Magn. Magn. Mater.,* 2005, **293**, 483.
37 C. Chen, H. Lai, C. Lin, J. Wang and R. Chiang, *Nanoscale. Res. Lett.,* 2009, **4**, 1343.

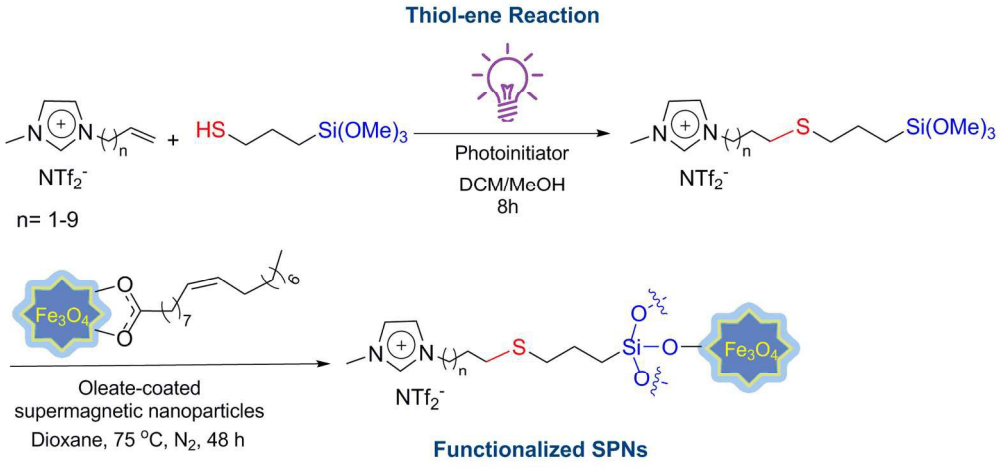

162x76mm (300 x 300 DPI)